

Supplementary Information

Engineering Recombinant Protein Sensors for Quantifying Histone Acetylation

Oscar F. Sanchez, Agnes Mendonca, Ana D. Carneiro, Chongli Yuan*

School of Chemical Engineering, Purdue University, 480 Stadium Mall Drive, West Lafayette, IN 47907, USA

* Corresponding author:

School of Chemical Engineering, Purdue University, 480 Stadium Mall Drive, West Lafayette, IN 47907, USA. Tel.: +1 7654945824; fax: +1 7654940805; E-mail: cyuan@purdue.edu

Table of Contents

Supporting Methods

Affinity measurements using bio-layer Interferometry (BLI)

Antibody immunostaining of transfected cells with protein sensors S-3

Table S1. Amino acid sequence of H3K14ac sensor. The epigenetic reader domain PB1(2) is in bold. Linker region is underlined. A cysteine (double underscored) was introduced before 6xHis-tag for fluorescent labeling. S-4

Table S2. Sequences of synthetic H3 peptides. S-5

Figure S1. An agarose gel (1.0%) showing digested (EcoRI and Sall) coding DNA plasmids of sensors. S-6

Figure S2. Left: A typical SDS-PAGE gel (18%) of cytoplasmic and nuclear extracts from HEK293T cells. Right: Western blotting image of nuclear extracts stained with anti-Histone H3 antibody (ab1791, Abcam, CA, US). S-7

Figure S3. Circular dichroism spectra of PB1(2) protein sensors with different numbers of tandem repeats. S-8

Figure S4. Typical autocorrelation curves and fitting results of the free protein sensor (o) and sensors mixed with nuclear extracts (V). Top panel shows the autocorrelation curve and the bottom one shows the fitting residuals. Typical γ^2 values of the fitting were found to be between 0.5 and 1.6. S-9

Figure S5. Diffusivity of rhodamine dyes mixed with nuclear extracts of varying H3K14ac concentrations. Data is presented as the mean value \pm SD, n = 3. S-10

Figure S6. Affinity measurements via bi-layer interferometry (BLI). **A.** Comparison of association and dissociation curves between the dimeric probe (2 μ M) and different H3 peptides. Only H3K14ac peptides exhibit a discernible association and dissociation curve, which can subsequently be used to determine the binding affinity. **B.** Binding affinity of the dimeric probe and H3K14ac was evaluated by varying the probe concentration from 0.25 to 2 μ M. The curves were then fitted globally and the K_d values was found to be 0.14 ± 0.02 μ M. S-11

Figure S7. Representative images of HEK293T cells transfected with *in situ* probes of PB1(2). S-12

Figure S8. Morphological comparison between untransfected and transfected cells. No significant difference was observed in the cell morphology visually.	S-13
Figure S9. Transfection efficiency (monitored as the percentage of fluorescent cells) of HEK293T cells transfected with the dimeric sensor. The efficiency reached a plateau value at ~ 24 hours after transfection and remained fairly constant till 72 hours after transfection. Insets: representative fluorescent and DIC overlay images collected using a 4× objective.	S-14
Figure S10. Comparison in the exponential phase growth of HEK293T (○, untransfected cells; and Δ, transfected cells with dimeric PB1(2)-mEGFP vector). The inset was the same data set plotted using logarithmic y-axis.	S-15
Figure S11. Dimeric PB1(2) sensor transfected into cells treated with NaB of varying concentrations.	S-16
Figure S12. Monomeric PB1(2) sensor transfected into cells treated with NaB in (A) and the CNF values for the same in (B). Data is showed as Mean ± S.E, n = 30 cells. Fluorescent probes exhibit a significant CNF value compared to the negative control (# : $p < 0.01$, ANOVA, Duncan's multiple-range test test). NaB, 5 mM, significantly (*: $p < 0.05$, ANOVA, Duncan's multiple-range test test) increased H3K14ac level compared to samples in absence of NaB.	S-17
Figure S13. Representative HEK293T cells transfected with the dimeric protein sensor and co-stained with H3K14ac-antibody. Cells were fixed for co-staining with antibody after exposure to the specific HDAC inhibitors ((A) NaB and (B) TSA).	S-18
Figure S14. CNF values and relative acetylation level obtained from the anti-H3K14ac antibody in HEK293T cells treated with NaB (A) or TSA (B) and transfected with the dimeric PB1(2) sensor. Data is showed as Mean ± S.E, n = 30 cells. *, $p < 0.05$; stands for a significant difference between the CNF value obtained with cells treated with the drug and the negative control, or untreated cells.	S-19

Supporting Methods

Affinity measurement using Bi-layer Interferometry (BLI)

To assess the specificity of the dimeric PB1(2) probe to H3K14ac, we used a bi-layer interferometry (BLI, OctetRed 384, ForteBio, Menlo Park, CA). Biotinylated histone peptides (with sequence detailed in **Table S2**) were loaded on streptavidin-activated capture biosensors (ForteBio, Menlo Park, CA). A binding buffer (HEPES, 25 mM, pH 7.5; NaCl, 150 mM; BSA, 0.1% w/v; and Tween 20, 0.05%v/v) was used to perform all binding assays. Sensors of concentrations ranging from 0.25 to 2.0 μ M were used to determine the binding affinity. The binding and dissociation curves were fitted using Octet software to determine the k_{on} and k_{off} , which subsequently can be used to determine K_d as k_{off}/k_{on} .

Antibody immunostaining of transfected cells with protein sensors

Transfected cells were seeded on poly-L-Lysine treated coverslips (No. 1.5 round coverslips, VWR, PA, US) and grown for 24 hours. Cells were then fixed using freshly prepared 4% paraformaldehyde in PBS for 20 minutes at room temperature, followed by 10 minutes of permeabilization with 0.2% Triton X-100 in PBS. Coverslips with fixed cells were then incubated with a primary antibody, anti H3K14ac (ab52946, Abcam, CA, US) at 4°C overnight. The cells were triple rinsed with PBS, followed by 1 hour of incubation at room temperature with the secondary antibody (an Alexa 564 coupled goat anti rabbit (ab175471, Abcam, CA, US)). A control well was prepared by incubating cells with the secondary antibody in absence of the primary to assess the non-specific activity of the secondary antibody

Table S1. Amino acid sequence of H3K14ac sensor. The epigenetic reader domain PB1(2) is in bold. Linker region is underlined. A cysteine (double underscored) was introduced before 6xHis-tag for fluorescent labeling.

Name	Amino acid sequence				
Monomeric H3acetyl- sensor	10	20	30	40	50
	MSPAYLKEIL	EQLLEAIVVA	TNPSGRLISE	LFQKLPSKVQ	YPDYYAIIKE
	60	70	80	90	100
	PIDLKTIAQR	IQNGSYKSIH	AMAKDIDLLA	KNAKTYNEPG	SQVFKDANSI
	110	120	130		
	KKIFYMKKAE	<u>IGSGGGGGGV</u>	DENLYFQGS	HHHHH	
	↑				
	(C)				
Dimeric H3acetyl- sensor	10	20	30	40	50
	MEFSPAYLKE	ILEQLLEAIV	VATNPSGRLI	SELFQKLPSK	VQYPDYYAII
	60	70	80	90	100
	KEPIDLKTIA	QRIQNGSYKS	IHAMAKDIDL	LAKNAKTYNE	PGSQVFKDAN
	110	120	130	140	150
	SIKKIFYMKK	AEIGSGGGGQ	FSPAYLKEIL	EQLLEAIVVA	TNPSGRLISE
	160	170	180	190	200
	LFQKLPSKVQ	YPDYYAIIKE	PIDLKTIAQR	IQNGSYKSIH	AMAKDIDLLA
	210	220	230	240	250
	KNAKTYNEPG	SQVFKDANSI	KKIFYMKKAE	IGSGGGGQLS	VGVDENLYFQ
	260				
	GSCHHHHHH				
Tetrameric H3acetyl- sensor	10	20	30	40	50
	MEFSPAYLKE	ILEQLLEAIV	VATNPSGRLI	SELFQKLPSK	VQYPDYYAII
	60	70	80	90	100
	KEPIDLKTIA	QRIQNGSYKS	IHAMAKDIDL	LAKNAKTYNE	PGSQVFKDAN
	110	120	130	140	150
	SIKKIFYMKK	AEIGSGGGGQ	FSPAYLKEIL	EQLLEAIVVA	TNPSGRLISE
	160	170	180	190	200
	LFQKLPSKVQ	YPDYYAIIKE	PIDLKTIAQR	IQNGSYKSIH	AMAKDIDLLA
	210	220	230	240	250
	KNAKTYNEPG	SQVFKDANSI	KKIFYMKKAE	IGSGGGGQFS	PAYLKEILEQ
	260	270	280	290	300
	LLEAIVVATN	PSGRLISELF	QKLPSKVQYP	DYYAIIKEPI	DLKTIAQRIQ
	310	320	330	340	350
	NGSYKSIHAM	AKDIDLLAKN	AKTYNEPGSQ	VFKDANSIKK	IFYMKKAEIG
	360	370	380	390	400
	SGGGGQFSPA	YLKEILEQLL	EAIVVATNPS	GRLISELFQK	LPSKVQYPDY
	410	420	430	440	450
	YAIIKEPIDL	KTIAQRIQNG	SYKSIHAMAK	DIDLLAKNAK	TYNEPGSQVF
	460	470	480	490	
	YMKKAEIGSG	GGGQLSVGVD	ENLYFQGSCH	HHHHH	

Table S2. Sequences of synthetic H3 peptides.

Peptide	Amino acid sequence
H3WT	ARTKQTARKSTGGKAPRKQLA-GGK(Biotin)
H3K14ac	ARTKQTARKSTGG-K(Ac) -APRKQLA-GGK(Biotin)
H3K9ac	ARTKQTAR-K(Ac)-STGGKAPRKQLA-GGK(Biotin)

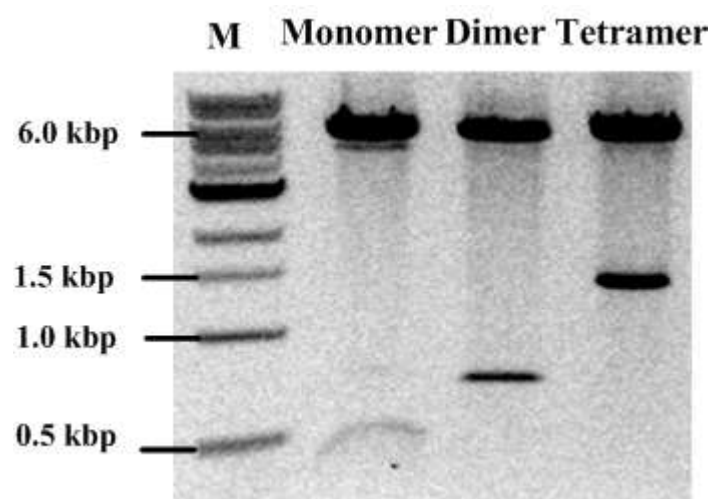


Figure S1. An agarose gel (1.0%) showing digested (EcoRI and Sall) coding DNA plasmids of sensors.

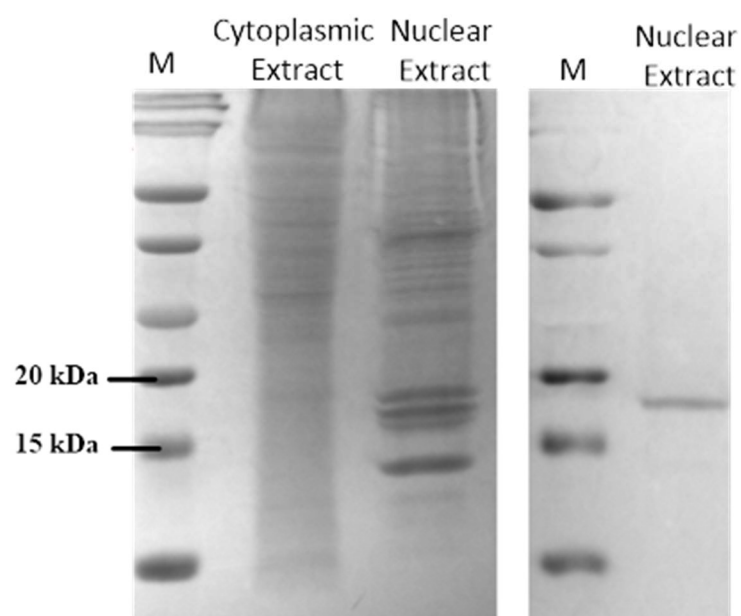


Figure S2. Left: A typical SDS-PAGE gel (18%) of cytoplasmic and nuclear extracts from HEK293T cells. Right: Western blotting image of nuclear extracts stained with anti-Histone H3 antibody (ab1791, Abcam, CA, US).

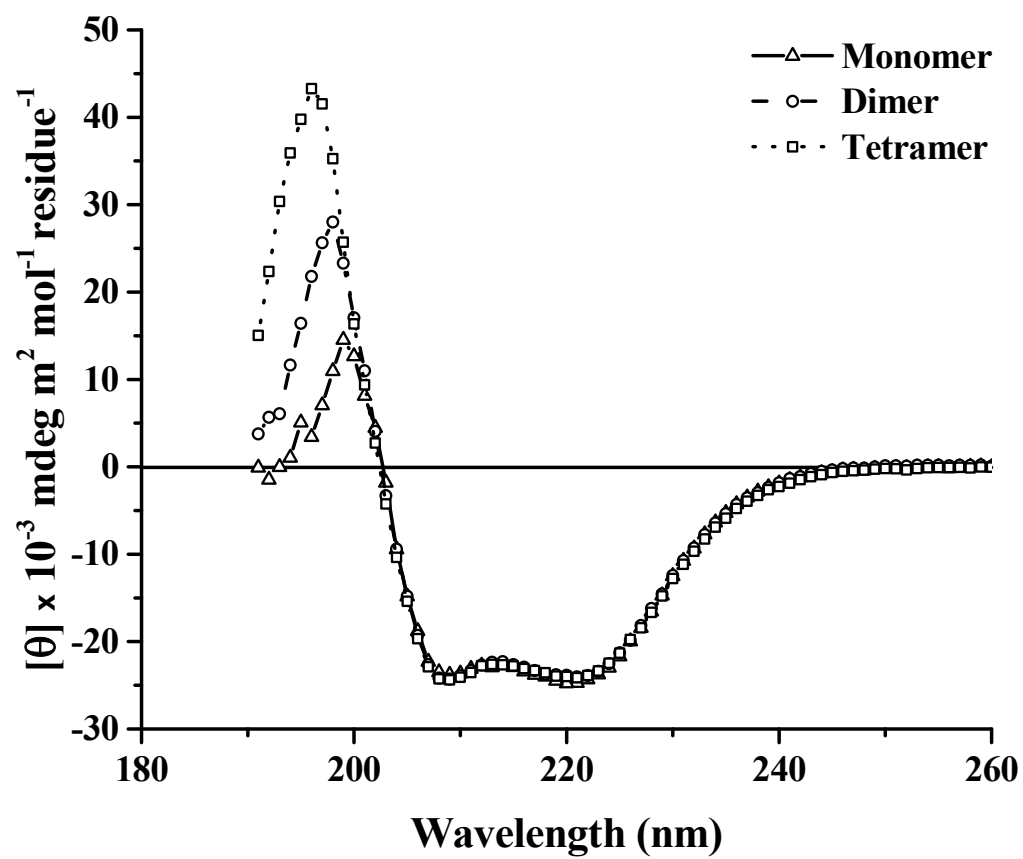


Figure S3. Circular dichroism spectra of PB1(2) protein sensors with different numbers of tandem repeats.

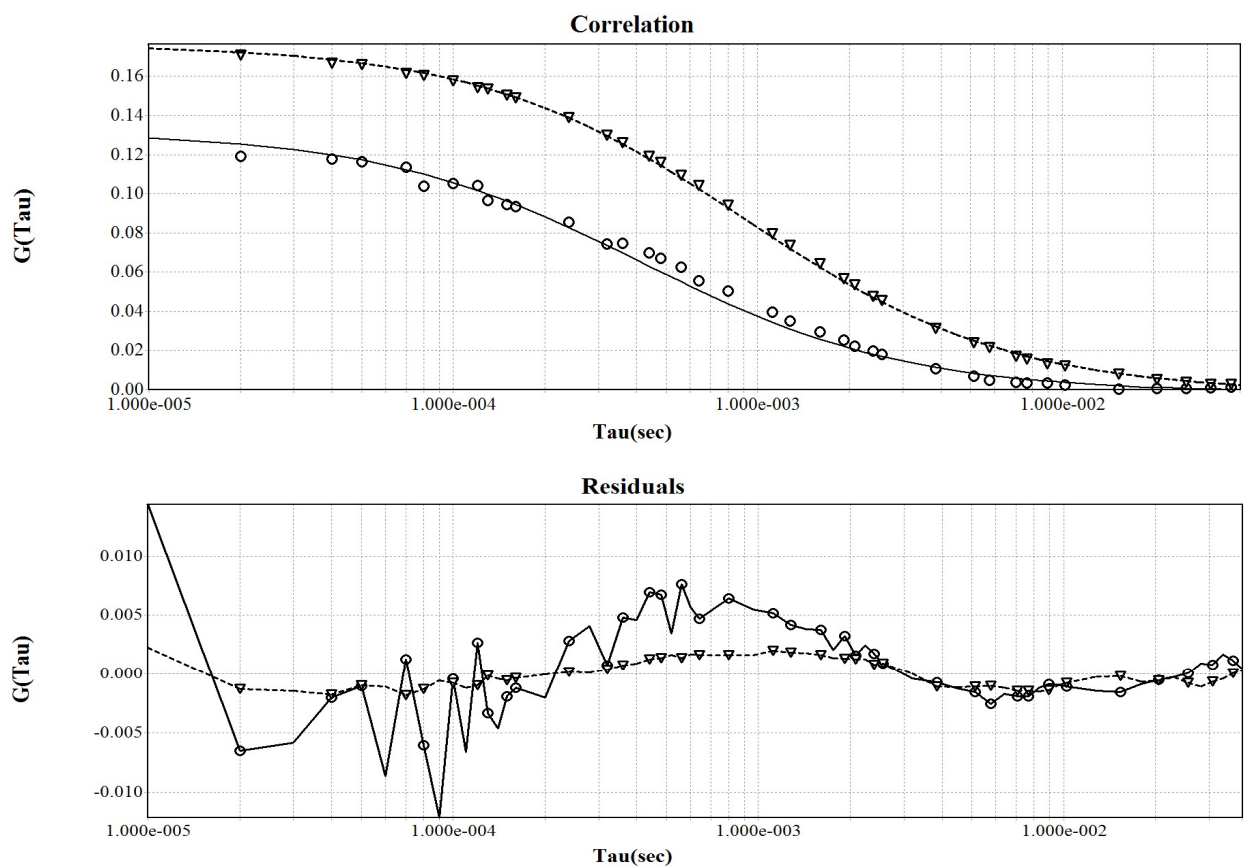


Figure S4. Typical autocorrelation curves and fitting results of the free protein sensor (o) and sensors mixed with nuclear extracts (∇). Top panel shows the autocorrelation curve and the bottom one shows the fitting residuals. Typical γ^2 values of the fitting were found to be between 0.5 and 1.6.

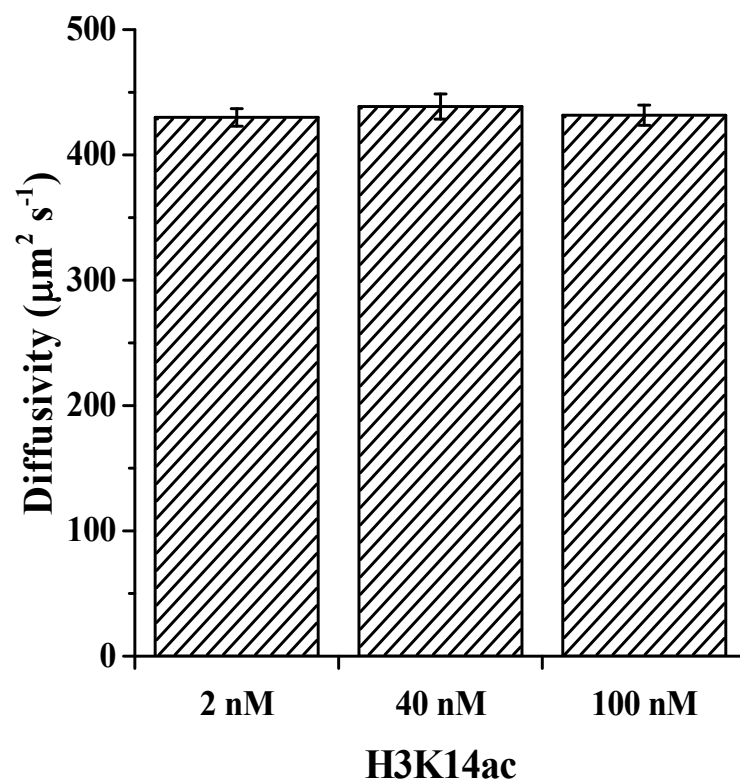
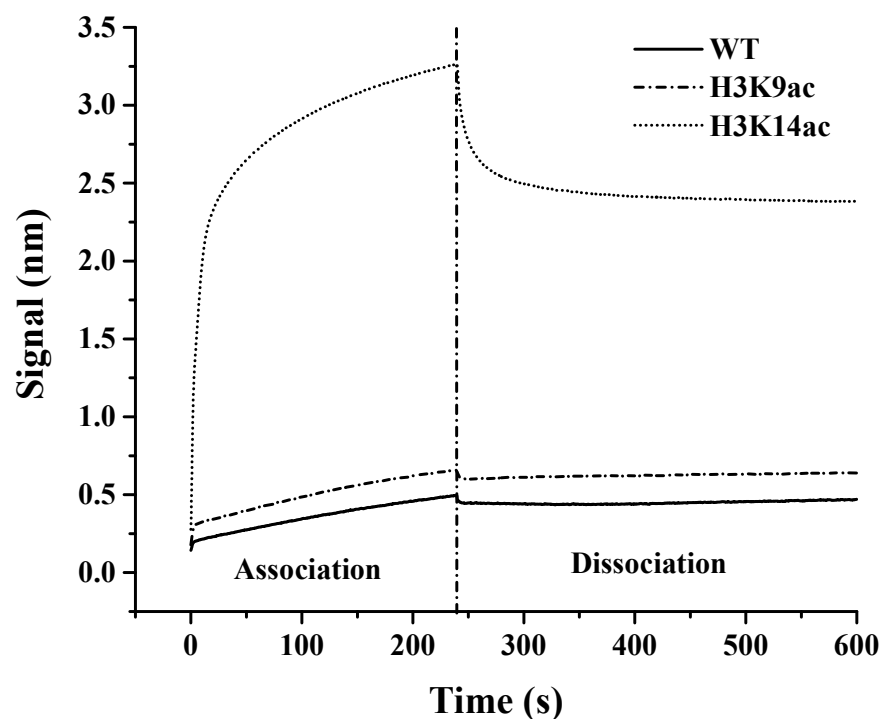


Figure S5. Diffusivity of rhodamine dyes mixed with nuclear extracts of varying H3K14ac concentrations. Data is presented as the mean value \pm SD, $n = 3$.

A.



B.

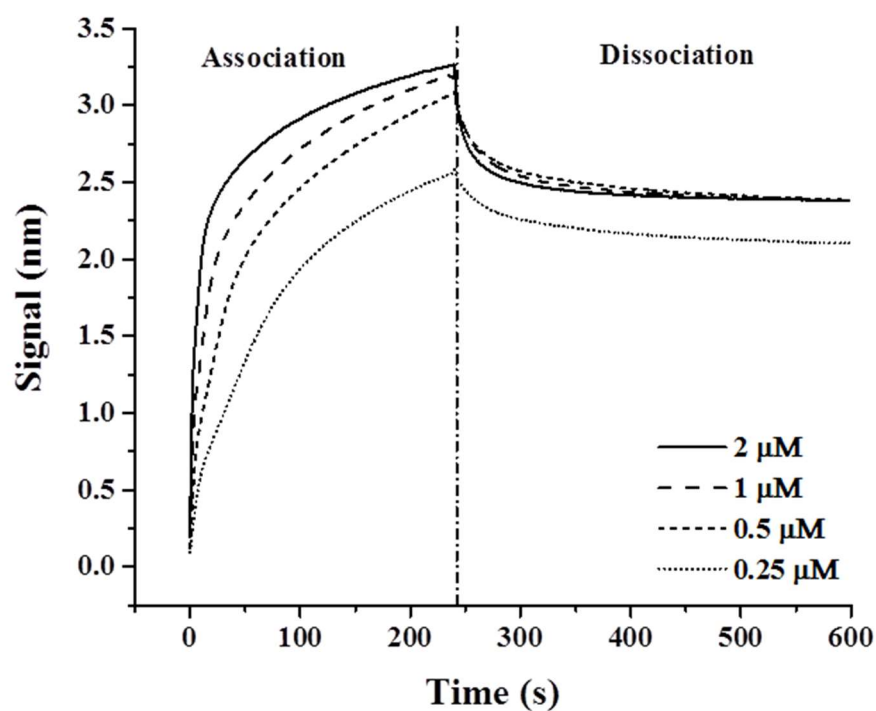


Figure S6. Affinity measurements via bi-layer interferometry (BLI). **A.** Comparison of association and dissociation curves between the dimeric probe (2 μ M) and different H3 peptides. Only H3K14ac peptides exhibit a discernible association and dissociation curve, which can subsequently be used to determine the binding affinity. **B.** Binding affinity of the dimeric probe and H3K14ac was evaluated by varying the probe concentration from 0.25 to 2 μ M. The curves were then fitted globally and the K_d values was found to be 0.14 ± 0.02 μ M.

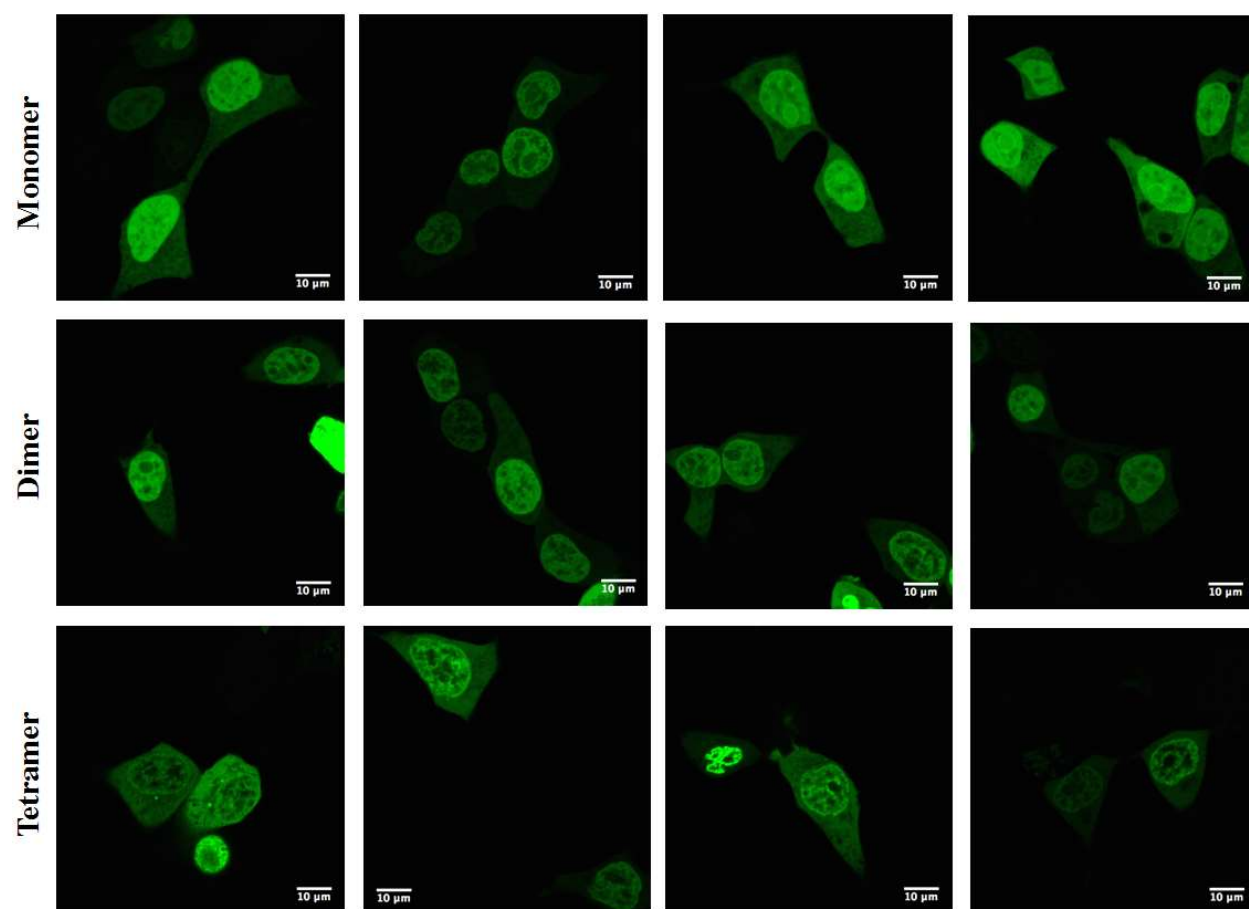


Figure S7. Representative images of HEK293T cells transfected with *in situ* probes of PB1(2).

Untransfected HEK293T
cells



Transfected HEK293T
cells with dimer PB1
sensor

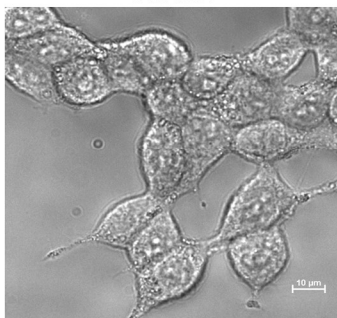


Figure S8. Morphological comparison between untransfected and transfected cells. No significant difference was observed in the cell morphology visually.

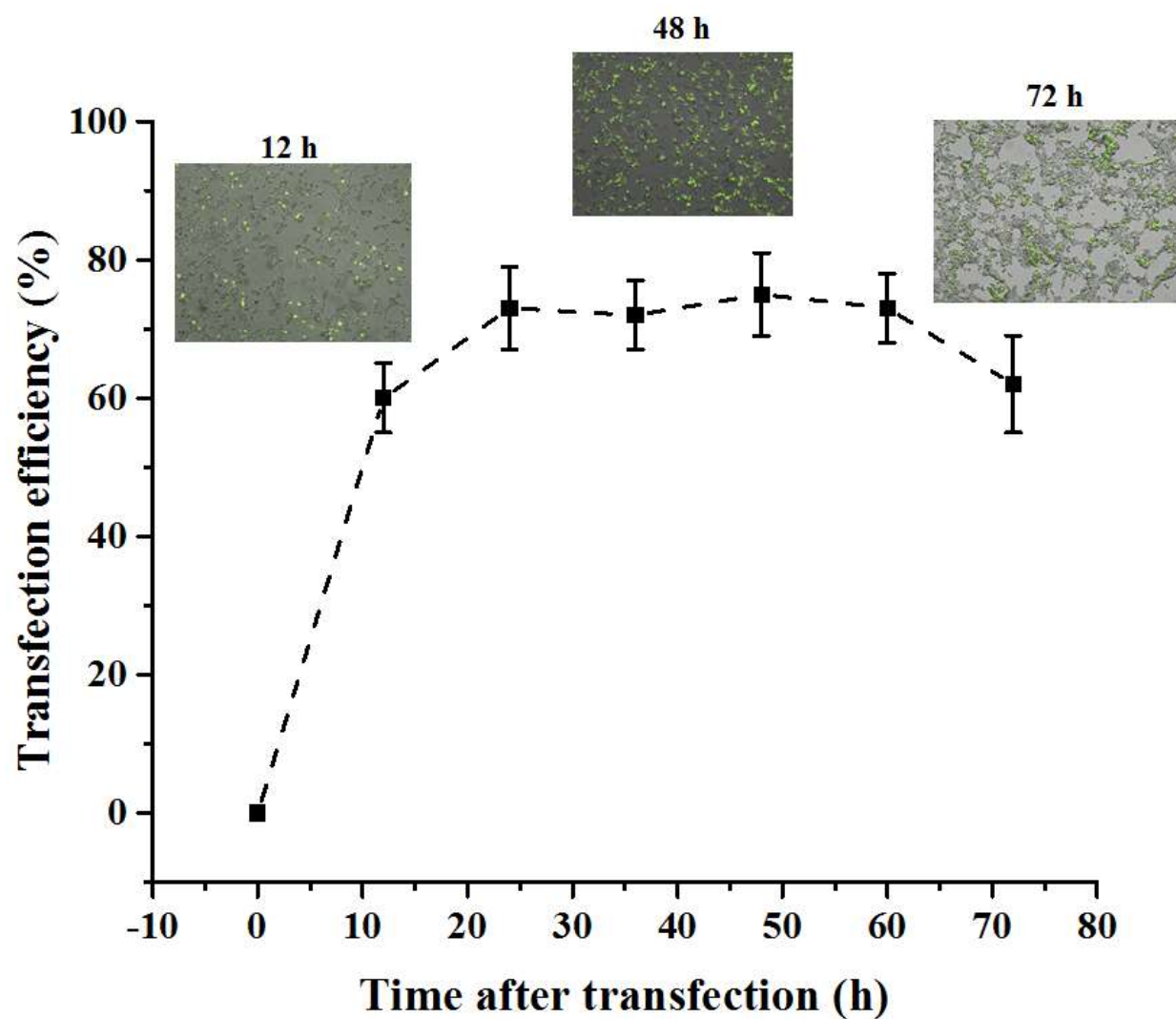


Figure S9. Transfection efficiency (monitored as the percentage of fluorescent cells) of HEK293T cells transfected with the dimeric sensor. The efficiency reached a plateau value at ~ 24 hours after transfection and remained fairly constant till 72 hours after transfection. Insets: representative fluorescent and DIC overlay images collected using a 4× objective.

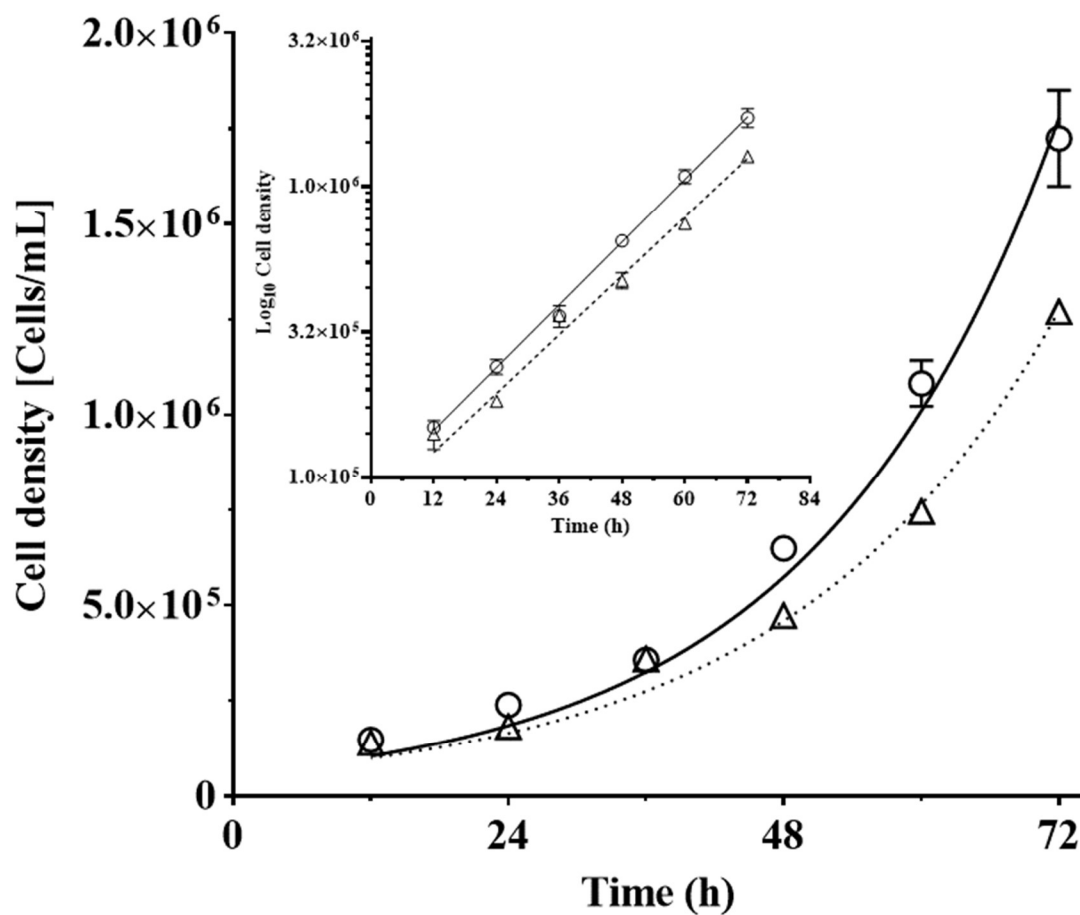


Figure S10. Comparison in the exponential phase growth of HEK293T (○, untransfected cells; and △, transfected cells with dimeric PB1(2)-mEGFP vector). The inset was the same data set plotted using logarithmic y-axis.

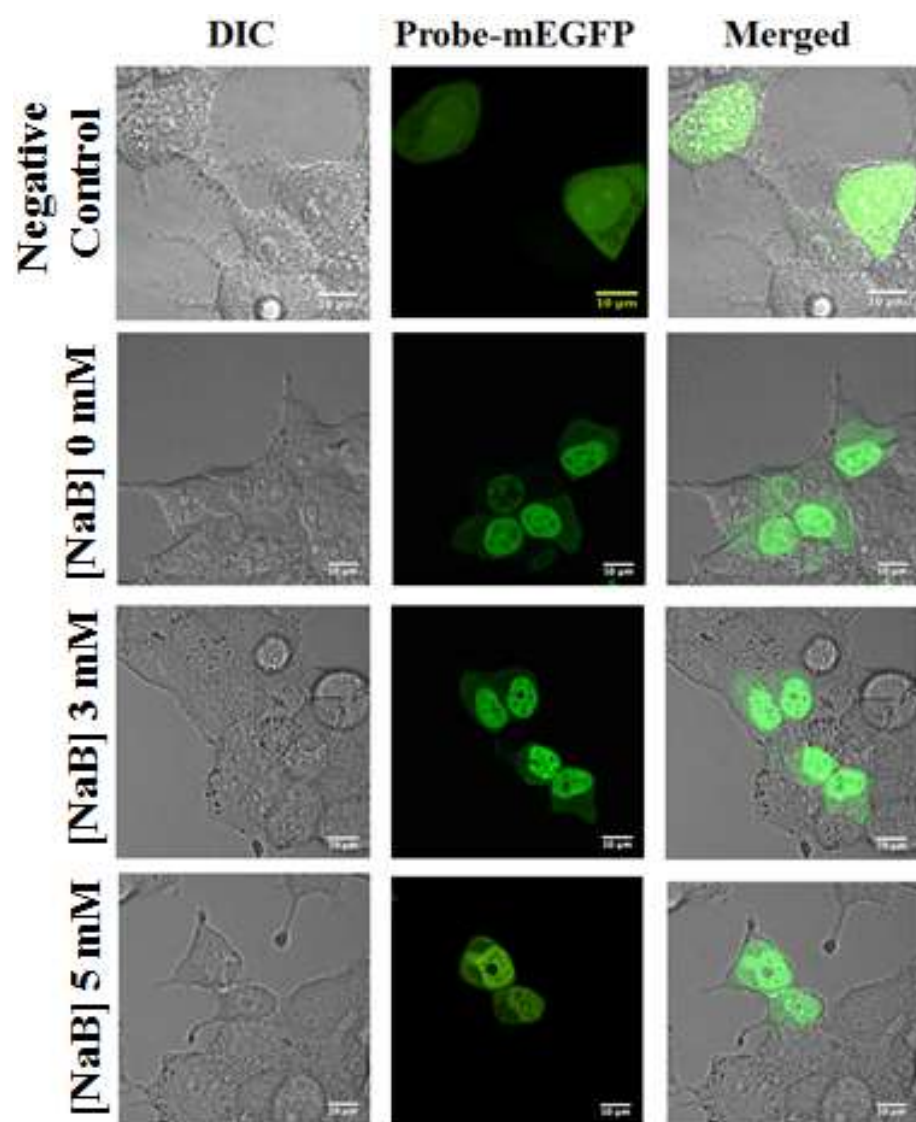


Figure S11. Dimeric PB1(2) sensor transfected into cells treated with NaB of varying concentrations.

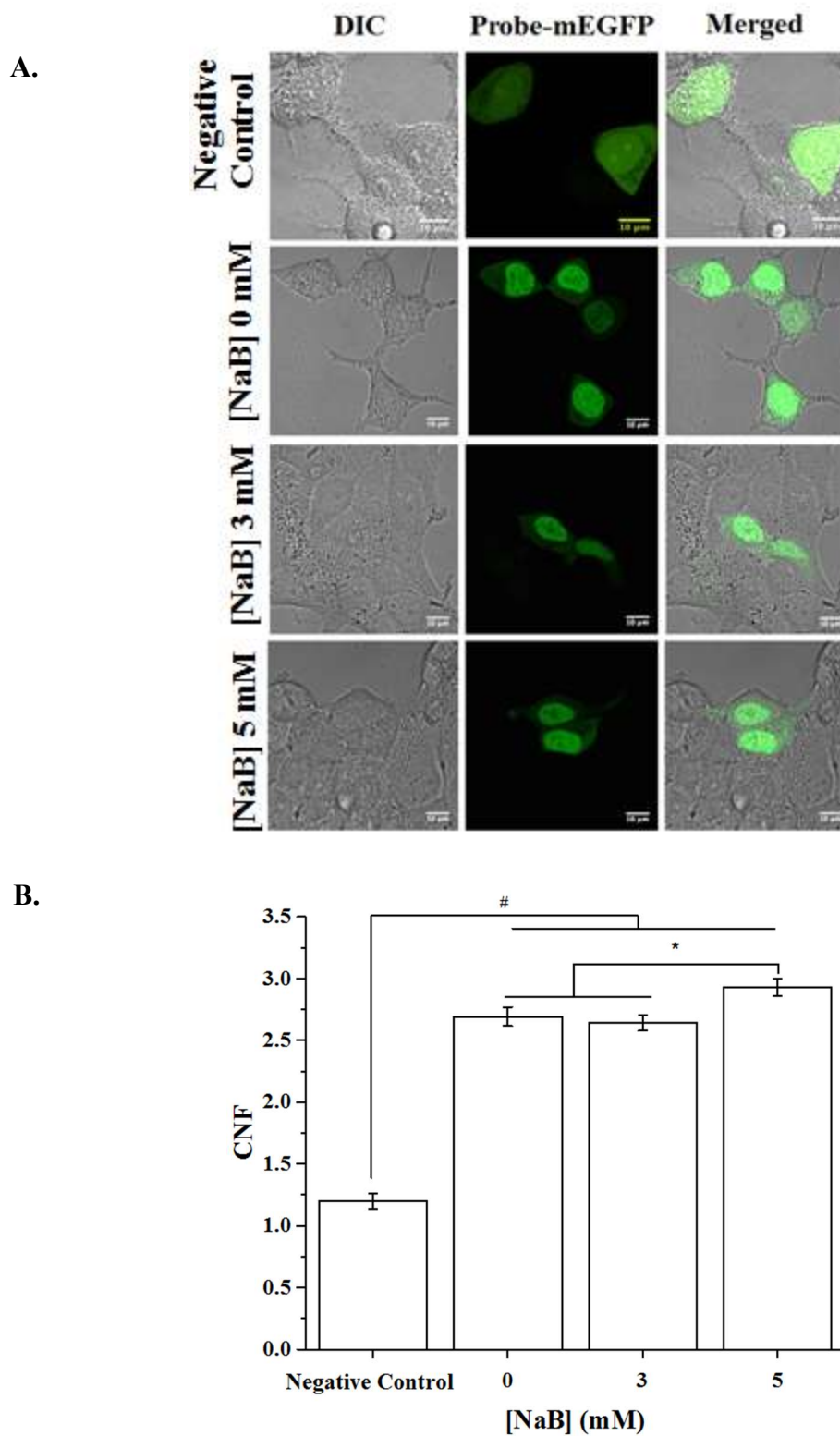


Figure S12. Monomeric PB1(2) sensor transfected into cells treated with NaB in (A) and the CNF values for the same in (B). Data is showed as Mean \pm S.E, $n = 30$ cells. Fluorescent probes exhibit a significant CNF value compared to the negative control (# : $p < 0.01$, ANOVA, Duncan's multiple-range test test). NaB, 5 mM, significantly (*: $p < 0.05$, ANOVA, Duncan's multiple-range test test) increased H3K14ac level compared to samples in absence of NaB.

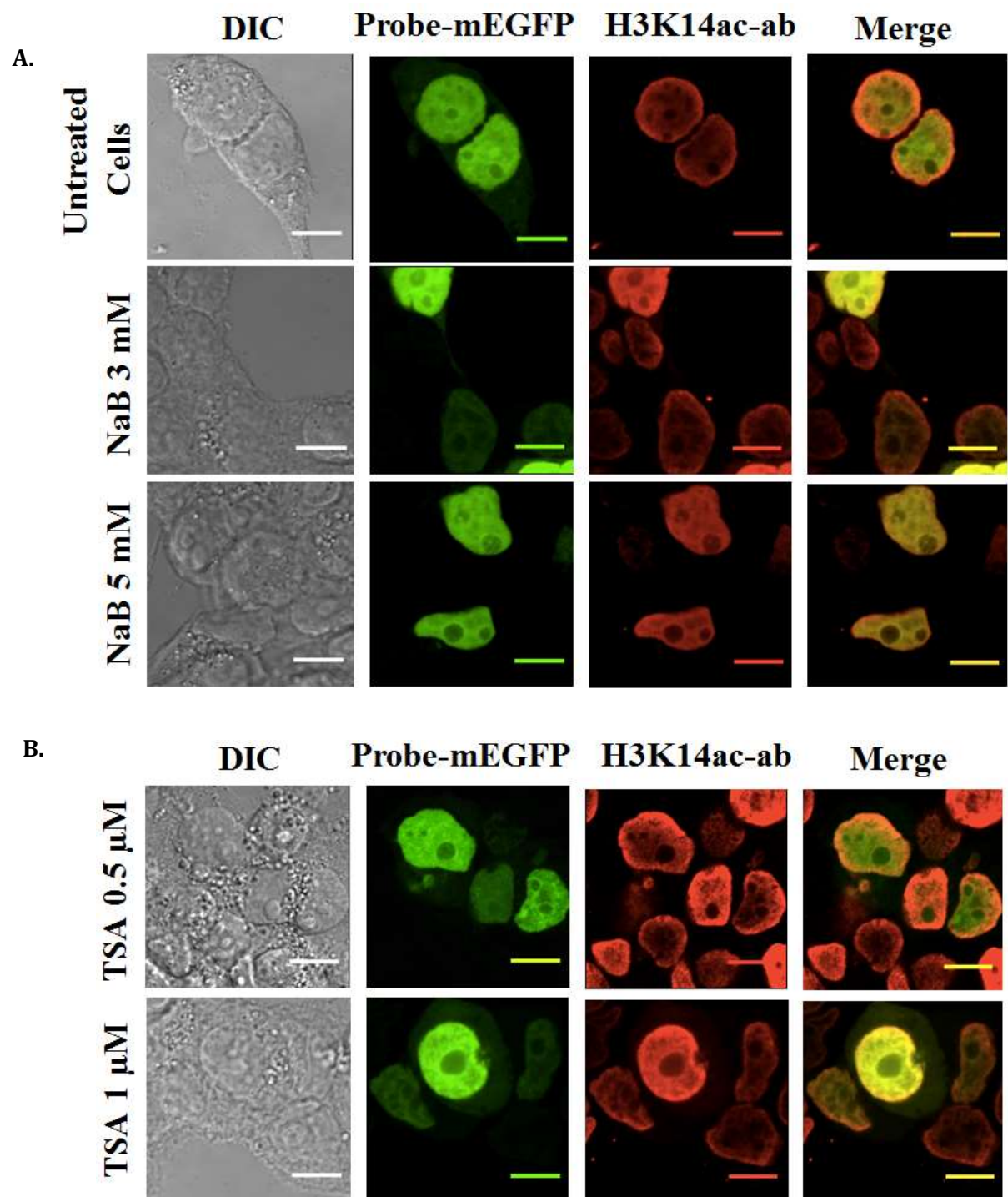


Figure S13. Representative HEK293T cells transfected with the dimeric protein sensor and co-stained with H3K14ac-antibody. Cells were fixed for co-staining with antibody after exposure to the specific HDAC inhibitors ((**A**) NaB and (**B**) TSA).

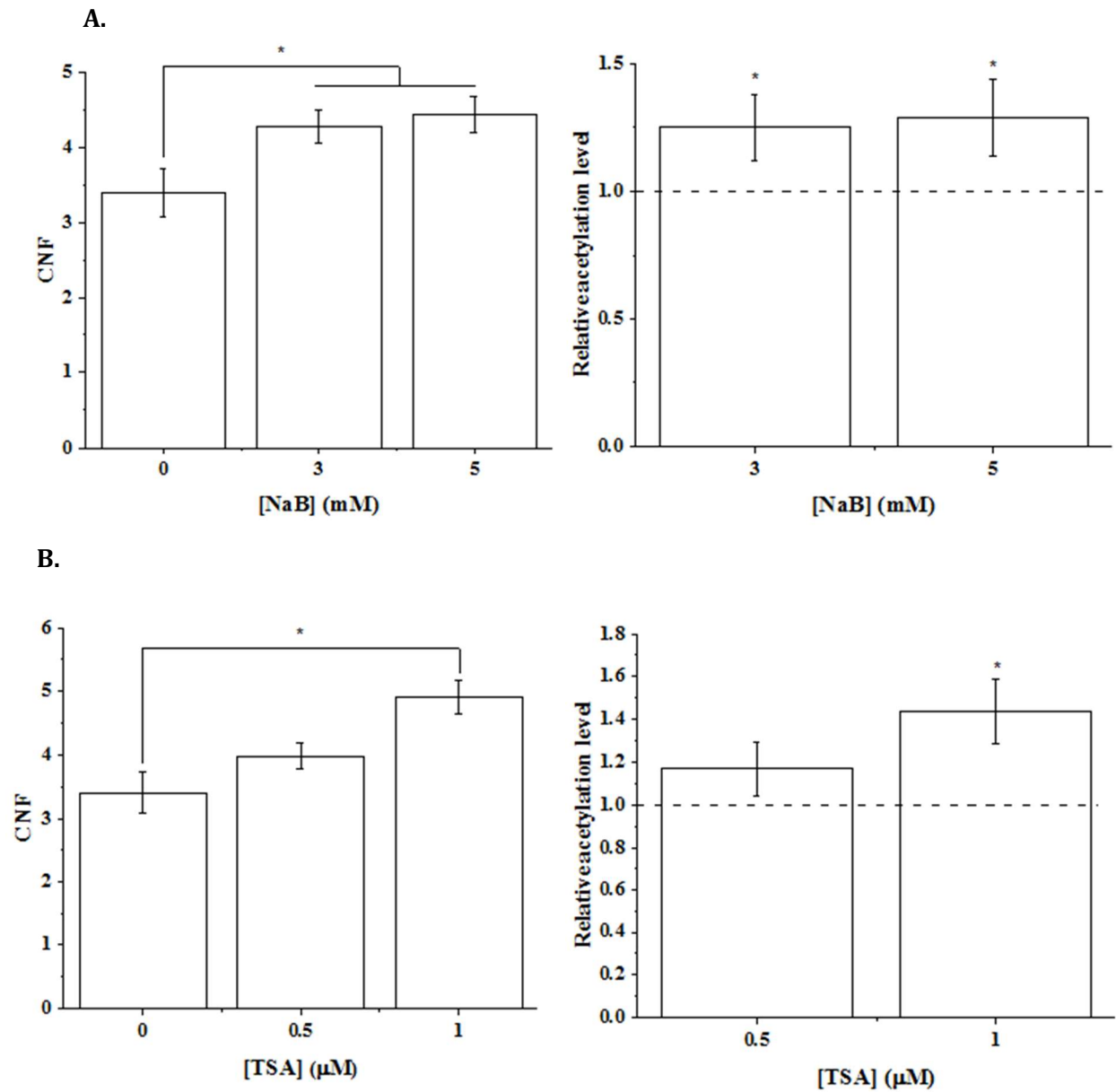


Figure S14. CNF values and relative acetylation level obtained from the anti-H3K14ac antibody in HEK293T cells treated with NaB (**A**) or TSA (**B**) and transfected with the dimeric PB1(2) sensor. Data is showed as Mean \pm S.E, $n = 30$ cells. *, $p < 0.05$; stands for a significant difference between the CNF value obtained with cells treated with the drug and the negative control, or untreated cells.